totes at 90° and 270°). If the gain were reduced to zero, the system would remain stable, but the steady-state error would be infinite, which is actually the case where no control is provided. A Bode diagram (Fig. 5) shows that the frequency response characteristics are poor because of the large time constant of the heating elements.

In order to compare the two control approaches that were proposed, the closed-loop transfer functions have been inversely transformed to the time domain. The tank pressure for the system presented in Fig. 4 where the input is a step of 24 v is of the form

$$\frac{\Delta P_s(t)}{A_1} = \frac{a_0}{\gamma(\alpha^2+\beta^2)} + \frac{(\gamma - a_0)e^{-\gamma t}}{\gamma[(\alpha-\gamma)^2+\beta^2]} + \left\{\frac{(a_0-\alpha)^2+\beta^2}{(\alpha^2+\beta^2)[(\alpha-\gamma)^2+\beta^2]}\right\}^{1/2} \cdot \frac{e^{-\alpha t}\sin(\beta t + \psi)}{\beta} \quad (14)$$

where $\psi = \tan^{-1}[\beta/(\alpha-\gamma) + \tan^{-1}(\beta/\alpha) + \tan^{-1}\beta/(a_0-\alpha)]$, $A_1 = -4.2$, $a_0 = 0.1$, $\gamma = 100$, $\alpha = 0.05$, and $\beta = 0.312$. Substituting these values,

$$\Delta P_s(t) = -4.2[0.0001 - 0.0001e^{-100t} + 0.03e^{-0.05t}\sin 0.312t] \quad (15)$$

The theoretical steady-state pressure deviation is −0.0004 psia, and thus the control system provides extremely tight control. The size of the heater could undoubtedly be reduced in an actual system unless higher flow rates were anticipated.

The second control presented in Fig. 3 includes a direct lead term input to the heating element and is also of the form of Eq. (14) where the constants are $A_1 = 5.0$, $a_0 = -40$, $\gamma = 100$, $\alpha = 0.05$, and $\beta = 0.312$. Evaluating the pressure response for the same system,

$$\Delta P_s(t) = 5[4 - 0.00014e^{-100t} - 4.06e^{0.05t}\sin(0.312t + 1.5)] \quad (16)$$

The steady-state pressure deviation would be 20 psia and thus the system is over-compensated. In order to apply this concept to this particular system, the gain K_7 of the lead term would have to be decreased and again the size of the heating element could be reduced.

Concluding Remarks

This volatile-liquid pressurization system can reduce system weight and required packaging space and eliminate gas flow control elements. Its disadvantages include the need for more electrical power, an electronic control package, and more complex propellant tank construction. Specific conclusions are as follows. 1) The simple pressure feedback control provides sufficient response and accuracy for low-thrust systems. 2) The direct heat control technique is required only for high-thrust or low-total-impulse systems where instantaneous pressure drops might occur; its need also depends upon the size of the tank or total impulse as well as the propellant flow rate. 3) A more detailed dynamic analysis is required in which the effects of heat transfer are considered as well as the nonlinear characteristics of the system; for zero-g applications, this analysis will be very difficult, hence a full-scale simulation of this system is required. 4) This technical approach can also be used in the study of volatile fluid transient behavior during storage in and expulsion from fixed or variable volume tanks, e.g., in a monopropellant propulsion system.

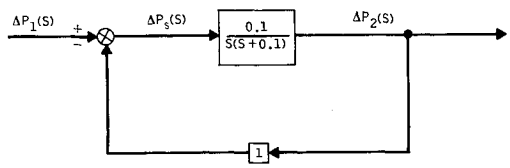

Fig. 4 Pressure control servosystem.

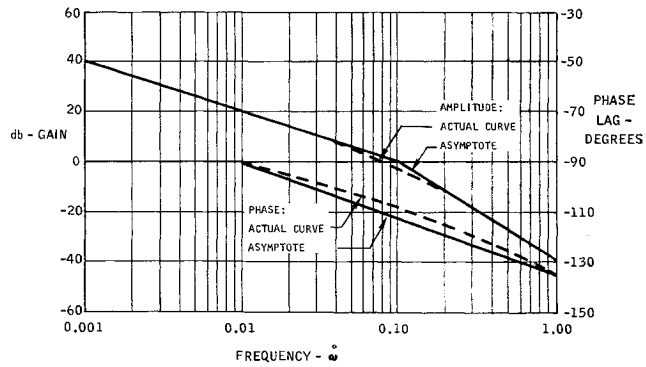

Fig. 5 Bode diagram.

Reference

[1] Kenny, R. J. and Friedman, P. A., "Chemical pressurization of hypergolic liquid propellants," J. Spacecraft Rockets **2**, 746–753(1965).

Parachute-and-Retrorocket Landing System for Vertical Descent

KENNETH E. FRENCH*
Lockheed Missiles and Space Company, Sunnyvale, Calif.

Nomenclature

c = rocket effective exhaust velocity, fps
C_D = parachute drag coefficient, dimensionless
D = parachute diameter, ft
g = acceleration of gravity, ft/sec²
k_j = const, dimensions as appropriate (j = 1–7)
m_b = mass of rocket propellant, slug
m_i = mass of rocket subsystem inert components, slug
m_0 = mass of payload, slug
m_p = mass of parachute, slug
m_r = mass of complete parachute subsystem, slug
M = total landing system mass, slug
t_b = rocket burning time, sec
T = rocket thrust, lb
v = specified touchdown velocity, fps
v_p = descent velocity on parachute, fps
π = numerical constant (= 3.141 . . .)
ρ = atmosphere mass density, slug/ft³

Introduction

A PROBLEM frequently encountered in recovery system design is that of providing a soft landing for a payload of known mass and strength. The landing systems used employ many basic types of deceleration devices; e.g., parachutes, retrorockets, crushable material, inflatable bags, and nose spikes. This paper considers a landing system that uses a parachute and a retrorocket in sequence, with particular attention to determination of a minimum weight system. Only vertical descent is considered. The vehicle is brought to an intermediate, stabilized rate of descent on the parachute, which is then cast free, and the retrorocket is ignited. Touchdown occurs at a specified velocity at the end of rocket burning. The parachute subsystem consists of the parachute assembly (canopy, lines and links, riser, pack), the

Received January 14, 1965; revision received March 17, 1965.
* Research Specialist. Member AIAA.

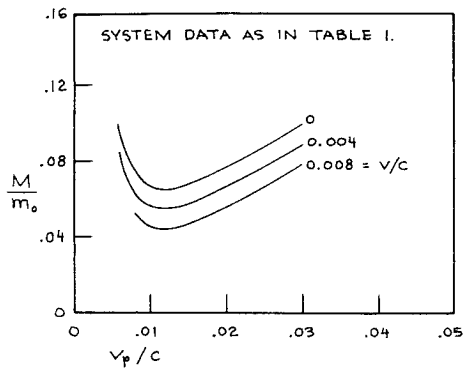

Fig. 1 Landing system mass vs parachute descent velocity for various touchdown velocities and fixed load factor.

sensing and actuating devices required for parachute deployment, and the structure required for stowage and attachment. The retrorocket subsystem consists of rocket propellant, rocket metal parts, the sensing and actuating devices required for parachute release and rocket ignition, and auxiliary attachment fittings or structure.

System Equations

For a given type and class of construction, parachute mass is very nearly proportional to the square of the parachute diameter,[1] i.e., $m_p \approx k_1 D^2$. The nonjettisonable elements of the parachute subsystem are such that the mass of the complete parachute subsystem may be expressed as a linear function of the mass of the parachute (e.g., Ref. 1, Fig. 22.92, pp. 22–130); thus, $m_r = k_2 + k_3 m_p$. With v_p the velocity of descent on the parachute, m_0 the payload mass, and $(m_i + m_b)$ the total rocket subsystem mass, the required size of the parachute is given by[1]

$$D^2 = k_4(m_0 + m_i + m_b + m_r)/v_p^2 \tag{1}$$

where $k_4 = 8g/\pi\rho C_D$. The rocket is specified by the parameters c, m_i, m_b, and t_b. For the problem considered, rocket subsystem inert mass is taken as $m_i = k_5 + k_6 m_b$, and rocket thrust as[2] $T = cm_b/t_b$. If the rocket thrusts against gravity

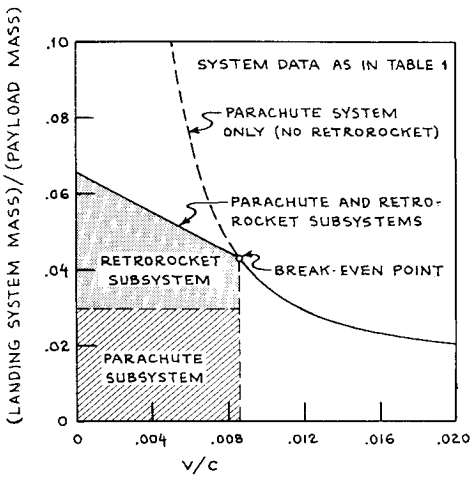

Fig. 2 Comparison of parachute-and-retrorocket and parachute-only landing systems.

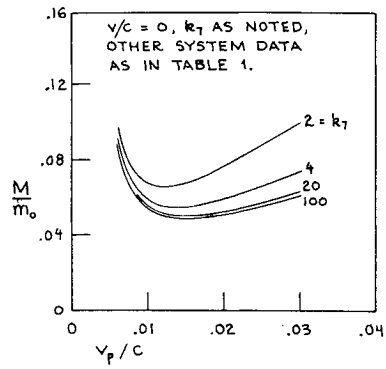

Fig. 3 Landing system mass vs parachute descent velocity for various load factors and fixed touchdown velocity.

in a vertical descent starting at velocity v_p, and if aerodynamic drag is neglected, the velocity at the end of burning will be[2]

$$v = v_p + gt_b - c\ln[(m_0 + m_i + m_b + m_r - m_p)/(m_0 + m_i + m_r - m_p)] \tag{2}$$

The rocket-burning program should utilize the highest allowable thrust so that the velocity gain due to gravity is minimized. Thus, if the payload will withstand a maximum load factor k_7, rocket thrust may be specified as

$$T = k_7 g(m_0 + m_i + m_r - m_p) \tag{3}$$

If it is assumed that the rocket propellant mass m_b is small relative to the mass of the rest of the system (say <10%), then one may use the approximation

$$\ln[(m_0 + m_i + m_b + m_r - m_p)/(m_0 + m_i + m_r - m_p)] \approx m_b/(m_0 + m_i + m_r - m_p) \tag{4}$$

The mass of the landing system is

$$M = m_i + m_b + m_r \tag{5}$$

With the use of the relationships developed through Eq. (3), the approximation of Eq. (4), and some rather heavy algebra, Eq. (5) may be put into the dimensionless form

$$\frac{M(v_p^2 - k_1k_3k_4)}{m_0c^2} = \frac{(k_2 + k_5)v_p^2}{m_0c^2} + \frac{k_1k_3k_4}{c^2} + \frac{k_7(1 + k_6)\left(\frac{v_p^2}{c^2}\right)\left(\frac{v_p^2 - k_1k_4}{c^2}\right)\left(1 + \frac{k_2 + k_5}{m_0}\right)}{(1 - k_7)\left[\frac{(v_p^2 - k_1k_3k_4)}{c^2}\right]\left[\frac{c}{v - v_p}\right] - \frac{k_6k_7(v_p^2 - k_1k_4)}{c^2} + \frac{k_1k_4k_7(1 - k_3)}{c^2}} \tag{6}$$

It may also be shown that

$$\frac{M(v_p^2 - k_1k_3k_4)}{m_0c^2} = \frac{(k_2 + k_5)v_p^2}{m_0c^2} + \frac{k_1k_3k_4}{c^2} + \frac{(1 + k_6)m_bv_p^2}{m_0c^2} \tag{7}$$

If the system constants c, v, and k_j are known, Eq. (6) may be used to obtain M/m_0 as an explicit function of v_p/c. Thus, Eq. (6) may be used to calculate the value of v_p/c for which landing system mass is a minimum for given values of c, v, and k_j. Unfortunately, Eq. (6) is so formidable that its physical implications are not readily apparent. These implications are best illustrated by a numerical example.

Numerical Example

Assume that a parachute-and-retrorocket landing system is required for a payload of 6 slugs mass which is to land on earth at sea level, that the maximum allowable load factor is $k_7 = 2$, and that conditions at initiation of parachute deployment and stability of descent requirements are such that a lightweight, ribbon-type parachute may be used. The input data required for the landing system calculation

Table 1 Input data for numerical example

Parameter and dimensions	Numerical value
Payload mass m_0, slug	6.0
k_1, slug/ft^{2a}	0.00087
k_2, slug^b	0.09
k_3 (dimensionless)^b	2.0
k_4, ft^4/slug-sec^{2c}	6.9×10^4
k_5, slug	0.03
k_6 (dimensionless)	0.25
k_7 (dimensionless)	2.0
c, fps	7746.

[a] Based on use of type II ribbon chute (Ref. 1, Fig. 22.86, pp. 22–126).
[b] See Ref. 1, Fig. 22.92, pp. 22–130.
[c] For $C_D = 0.5$, $\rho = 0.00238$ slug/ft^3, and $g = 32.2$ ft/sec^2.

are listed in Table 1; v and v_p are left as free variables in the problem.

The results are shown in Fig. 1, in which the ordinate is the ratio of landing system mass to payload mass M/m_0, the abscissa is the ratio of parachute descent velocity to rocket exhaust velocity v_p/c, and each curve is associated with a different value of the ratio of touchdown velocity to rocket exhaust velocity v/c. These results may be used in turn to obtain a plot of M_{opt}/m_0 vs v/c, where M_{opt} is the minimum landing system mass corresponding to the data of Table 1 and to a given v (Fig. 2). Also shown in Fig. 2 is a curve of dimensionless parachute subsystem mass m_r/m_0 vs v/c for a landing system using a parachute subsystem only. (The mass equation for a parachute-only landing system is obtained with the condition that $m_i = m_b = 0$ in the appropriate equations.) That part of Fig. 2 applicable to a parachute-and-retrorocket landing system has been shaded to indicate the portions of landing system mass associated, respectively, with the parachute and retrorocket subsystems. For $v/c < 0.0086$, the parachute-and-retrorocket landing system is lighter.

Variations in M/m_0 resulting from variations in the load factor k_7 can be determined by fixing v/c and calculating a curve of M/m_0 vs v_p/c for each value assumed for k_7. The results of such calculations for a constant value of $v/c = 0$ are shown graphically in Fig. 3.

Discussion

For the example, Figs. 1 and 2 show that the parachute descent velocity associated with M_{opt} and the parachute subsystem portion of M_{opt} remain sensibly constant with respect to variations in v. Thus, the minimum-mass landing system is achieved essentially by letting the parachute subsystem operate at a fixed "optimum" descent velocity and by requiring that the retrorocket subsystem handle any remaining velocity decrement. Figures 2 and 3 show that M_{opt} increases with decreasing touchdown velocity, increases with decreasing load factor, and is insensitive to changes in load factor at relatively high load factors. These results are intuitively evident; however, the figures show the variations quantitatively.

As stated previously, it is desirable to use a high load factor in order to minimize velocity gain due to gravity during the rocket-burning phase of the descent. Also, a high load factor permits use of a relatively short probe if a mechanical probe arrangement is used to sense the altitude for ignition of the retrorocket. However, from an over-all system point of view, one would not use a higher load factor for the rocket phase of the descent than would prevail during other phases of the flight. Also, too high a load factor may, when coupled with subsystem component tolerances, give too little time for effecting release of the chute and ignition of the retrorocket.

For some recovery system designs, parachute weight may depend on conditions at initiation of deployment, rather than on terminal conditions, as was assumed in this analysis. Such a case could be accounted for by use of a heavier type of chute (e.g., Ref. 1, Fig. 22.86, pp. 22–126). In general, however, the weight of a final descent parachute does indeed depend on terminal conditions, since stringent initial conditions may be handled by reefing[3] or by the addition of a small, auxiliary, initial deceleration parachute to the system.

Finally, the analysis of this paper has been conducted with a view to weight optimization only, and other system factors may override weight considerations as such. For example, the relative reliabilities of the parachute-only and the parachute-and-retrorocket landing systems will influence system design.

References

[1] Knacke, T. W., "Recovery systems and equipment," *Handbook of Astronautical Engineering* (McGraw-Hill Book Co., Inc., New York, 1961), pp. 22-123–22-131.

[2] Sutton, G. P., *Rocket Propulsion Elements* (John Wiley and Sons, Inc., New York, 1956), 2nd ed., pp. 17, 380.

[3] "Performance of and design criteria for deployable aerodynamic decelerators," Wright-Patterson Air Force Base Aeronautical Systems Div., ASD-TR-61-579, pp. 183–188 (December 1963).

A High-Vacuum Calibration System

F. G. Sherrell* and A. J. Mathews†
ARO, Inc., Arnold Air Force Station, Tenn.

Ionization gages and mass spectrometers must be carefully calibrated before they can be used to indicate total and partial pressures in space simulation chambers. Two possible approaches to this vacuum calibration problem[1] are: 1) a standard vacuum gage might be adopted if one were available (however, the McLeod gage has inadequate accuracy at pressures below 10^{-5} torr, and ionization gages that provide adequate standardization for industrial processing purposes do not satisfy the requirement for calibration against an absolute standard); and 2) absolute, reproducible low pressures can be generated by the multiple-expansion method, the calculated rate-of-rise technique, or one of the various calibrated conductance techniques.[1–3] The vacuum calibration system described here employs a conductance technique using porous molecular leaks in series with a circular orifice.

Technique and System Description

Gas is introduced into the test region (Fig. 1) through a leak of conductance C_1, and the resulting test-region pressure P_2 is calculated by equating the flow through the leak to the flow through the orifice C_2 at equilibrium. Thus

$$C_1(P_1 - P_2) = C_2(P_2 - P_3) \quad (1)$$

In this expression P_1 is the leak forepressure, and P_3 is the

Presented at the AIAA Space Simulation Testing Conference, Pasadena, Calif., November 16–18, 1964 (no preprint number; published in bound volume of preprints of the meeting); revision received March 29, 1965. The research reported in this note was sponsored by the Arnold Engineering Development Center, Air Force Systems Command, under Contract AF 40(600)-1000 with ARO, Inc. Further reproduction is authorized to satisfy needs of the U. S. Government. The authors are pleased to acknowledge the valuable consultations with C. E. Normand of Oak Ridge, Tennessee and C. L. Owens of ARO, Inc.

* Engineering Physicist.
† Electrical Engineer.